

Pishgu: Universal Path Prediction Architecture through Graph Isomorphism and Attentive Convolution

Ghazal Alinezhad Noghre*
galinezh@uncc.edu

Vinit Katariya*
vkatariy@uncc.edu

Armin Danesh Pazho
adaneshp@uncc.edu

Christopher Neff
cneff1@uncc.edu

Hamed Tabkhi
University of North Carolina at Charlotte
NC, USA
htabkhiv@uncc.edu

Abstract

Path prediction is an essential task for several real-world real-time applications, from autonomous driving and video surveillance to environmental monitoring. Most existing approaches are computation-intensive and only target a narrow domain (e.g., a specific point of view for a particular subject). However, many real-time applications demand a universal path predictor that can work across different subjects (vehicles, pedestrians), perspectives (bird's-eye, high-angle), and scenes (sidewalk, highway). This article proposes Pishgu, a universal graph isomorphism approach for attentive path prediction that accounts for environmental challenges. Pishgu captures the inter-dependencies within the subjects in each frame by taking advantage of Graph Isomorphism Networks. In addition, an attention module is adopted to represent the intrinsic relations of the subjects of interest with their surroundings. We evaluate the adaptability of our approach to multiple publicly available vehicle (bird's-eye view) and pedestrian (bird's-eye and high-angle view) path prediction datasets. Pishgu's universal solution outperforms existing domain-focused methods by producing state-of-the-art results for vehicle bird's-eye view by 42% and 61% and pedestrian high-angle views by 23% and 22% in terms of ADE and FDE, respectively. Moreover, we analyze the domain-specific details for various datasets to understand their effect on path prediction and model interpretation. Although our model is a single solution for path prediction problems and defines a new standard in multiple domains, it still has a comparable complexity to state-of-the-art models, which makes it suitable for real-world application. We also report the latency and throughput for all three domains on multiple embedded processors.

*G. Alinezhad Noghre and V. Katariya have equal contribution.

1. Introduction

Path prediction is an essential task in many real-world computer vision applications [35, 10], which needs real-time analysis of the subjects and proper proactive decisions. It deals with predicting the paths of the subjects in a frame based on their movement in past few seconds. A wide range of computer vision applications in pedestrian safety, transportation safety, intelligent traffic monitoring, and video surveillance needs an accurate, robust, and efficient path-prediction algorithm. The applications vary from bird's-eye views for drone-related and environmental monitoring applications to high-angle views for safety, traffic monitoring, and surveillance application for humans and moving vehicles.

Path prediction as a whole has a set of universal objectives. All path prediction algorithms are tasked to determine future trajectories based on the current/past trajectories across all subjects of interest (e.g., vehicles or people). The algorithms must capture the individual behaviors of all subjects and their complex interactions with respect to each other (social interaction) and the surrounding environment (environmental interaction). Within these similar objectives, each context/domain often imposes its unique requirements and nuances. For instance, a busy highway has many hundreds of vehicles in a scene, and their speeds will be around 30 meters per second [5, 6]. The camera angles also cover a large field of view from a very high angle to capture the fast-moving vehicles early enough to generate accurate predictions. In contrast, a surveillance camera overlooking a campus sidewalk will rarely have over a hundred people, who also move much slower, around 1.4 meters per second [3]. The camera will also be much closer to the ground, making the view less bird's-eye and more high-angle.h

We observe a proliferation of algorithms [32, 31, 23, 42,

27] that try to optimize the path prediction for a single context and perspective. Most existing approaches focus on an isolated domain and fail to evaluate the generality of their solution over different contexts and domains [4, 25, 31]. It is rare to see approaches that predict for both vehicles and pedestrians [30, 4], and it is only recently that select pedestrian focused approaches started using both bird’s-eye and high-angle views [11, 22, 21, 20, 17]. When it comes to real-world deployment and applications, a general domain-agnostic approach that can accurately predict both pedestrians and vehicles across different views and perspectives is highly desirable.

At the same time, path prediction is inherently a real-time task with a demand for one single accurate prediction for all subjects of interest at any point of time [27, 19]. However, many existing path predictions rely on a spectrum of predictions with significantly large model sizes. Most works in this context predict multiple future trajectories and choose the best to assess their accuracy and performance [42, 26, 36]. Predicting the spectrum of possibilities and picking the best one makes the real-world implementation for real-world applications with the demand for a single prediction per each subject infeasible.

This paper introduces Pishgu¹, a domain-agnostic path prediction approach for a wide range of applications. Similar to [27, 24], Pishgu borrows Graph Isomorphism Network (GIN) [40] formulation for capturing the relative information between subjects. In addition to GIN, Pishgu goes further by leveraging attention mechanisms to create robustness against noisy data, a large number of parallel path predictions, and environmental alterations. With this, Pishgu sets a new state-of-the-art (SotA) for two important path prediction domains, vehicle bird’s-eye view, and pedestrian high-angle view. In the vehicle domain, Pishgu achieves up to $2\times$ improvement in Root Mean Squared Error and a $1.7\times$ and $2.5\times$ improvements in Average Displacement Error (ADE) and Final Displacement Error (FDE) respectively, when compared to the current SotA approach. In the pedestrian high-angle view domain, Pishgu is able to improve both ADE and FDE by $1.3\times$. Additional evaluation on real-world embedded processors demonstrates Pishgu’s suitability for real-time applications, with a sample latency across all domains under 4 milliseconds. In the pedestrian domain, Pishgu achieves between 50 and 190 FPS on the embedded processors.

In summary, this paper has the following contributions:

- We introduce Pishgu; a domain-agnostic path predictor with a novel formulation based on the graph isomorphism network and attention mechanism for a wide range of applications that demand robust, accurate, and lightweight path prediction across different subjects

and views.

- We provide a comprehensive domain analysis across the major datasets and domains in vehicle and pedestrian path prediction to better understand the variations in Pishgu’s accuracy with respect to the richness and characteristics of datasets within each domain.
- We provide a comprehensive evaluation of Pishgu across multiple domains, with respect to each domain’s characteristics, and demonstrate Pishgu’s SotA accuracies in two major domains: (1) Pedestrian high-angle view, (2) Vehicles bird’s-eye view.
- To verify Pishgu’s suitability for real-time applications, we report the latency and throughput on the Nvidia Carmel and ARM Cortex-A57 processors; two low-power embedded processors commonly used in real-world systems.

2. Related Work

In the following, we review existing path prediction approaches in three primary domains: (1) Vehicle Bird’s-eye View, (2) Pedestrian Bird’s-eye View, and (3) Pedestrian High-angle View.

2.1. Vehicle Bird’s-eye View Path Prediction

Many approaches focus on predicting the future path of vehicles in a bird’s-eye view setting on highways [31, 23, 19]. These methods use real-world coordinates and measure the error in meters. CS-LSTM [7], a pioneering paper in vehicle path prediction used Long Short-term Memory (LSTM) encoder-decoder model with convolutional social pooling. GRIP++ [19], an extension to [18], uses fixed and dynamic graphs with an LSTM encoder-decoder model to grasp the surrounding dynamics and predict the trajectories of the vehicles in a scene. STA-LSTM [23] utilizes Spatio-temporal attention along with LSTM to predict a vehicle’s future path and increase the explainability of the predictions. [32] incorporates the ego vehicle’s planned path into the prediction of the surrounding vehicles’ future paths to enhance predictions in an autonomous vehicle setting. [41] uses a graph self-attention network to understand both spatial and temporal interactions among the many vehicles in a scene and is used for both path prediction and lane-changing classification. In [28], a three-channel framework with a heterogeneous edge-enhanced graph attention network is proposed to deal with the inherent heterogeneity of the different vehicles in a given scene. DeepTrack [12] introduces temporal and depthwise convolutions to provide a more robust encoding of vehicle dynamics while reducing computation and parameters, resulting in a faster, lightweight network with competitive accuracy. [31] proposed

¹Pishgu means fortune teller in the Persian language.

recently, utilizes a graph-based spatial-temporal convolutional network and a gated recurrent unit to predict future vehicle paths. They also propose a weighted adjacency matrix for understanding the intensity of influence between different vehicles.

2.2. Pedestrian Bird’s-eye View Path Prediction

Similar to vehicle path prediction, pedestrian path prediction often relies on a bird’s-eye view of real-world coordinates and measures the error in meters. Many works have tackled the problem of path prediction in recent years. Most of them only focus on multi-future path prediction [42, 44, 26, 36], and evaluate the model by picking the best out of several predicted paths. However, in real-time scenarios generating multiple outputs per subject is not insightful. Therefore, we mostly focus on the works that perform single future path prediction analysis. [1] uses LSTM modules to jointly predict the trajectories of all pedestrians in a scene. [34] introduces attention to model the importance of social interactions without relying on proximity. Trajectron++ [30], designed for integration with robotic frameworks, utilizes a graph-structured recurrent model and heterogeneous data. While the focus is on pedestrians, Trajectron++ also predicts the future paths of vehicles to better understand how pedestrians might react to them. CARPe Posterum [27] utilizes graph isomorphism networks and a lightweight Convolutional Neural Network (CNN) for path prediction, considerably reducing computation and model size, targeting real-time applications. SSAGCN [25] uses an attention graph convolutional network and defines a new formulation to consider both social interactions as well as environmental factors as they can change the path that pedestrians may choose.

2.3. Pedestrian High-angle View Path Prediction

As applications that require pedestrian path prediction do not always have access to bird’s-eye view cameras or real-world coordinates, many works have moved to use high-angle views, and pixel space (x, y) coordinates in addition to the traditional bird’s-eye view model. [17] integrates multiple graph-based spatial transforms and trajectory smoothing to both exploit temporal information and correct temporally inconsistent trajectories. SimAug [20] utilizes synthetic data to improve the robustness of learned representations with the goal of better generalization in unseen contexts. Peeking into the Future [22] proposes a multi-task model to predict both future paths and future activities, with the belief that understanding the future activity is highly informative to the future path. Multiverse [21] builds upon [22] by introducing synthetic data and multi-scale location information and replacing graphs with Recurrent Neural Networks (RNNs). ScePT [4] proposes predicting paths at the scale of “cliques” rather than for each

individual. Similar to Trajectron++ [30] and GAIN [24], ScePT predicts trajectories for both vehicles and pedestrians.

Some of the works have tried to tackle the problem of path prediction in more than one domain [24, 30, 22]. However, none of them evaluate their model on all three discussed domains.

3. Pishgu

Path prediction in different domains inherently depends upon the position, past movements, and end goals of the subjects present in a scene. The end goals and movement patterns vary significantly between different environments (highway, sidewalk, etc.) and subjects (vehicle, pedestrian). However, graph neural networks assist in understanding the varying patterns in the respective domains. Pishgu uses GIN to grasp the inter-dependencies of all subjects in a scene. Attention-based convolutions are utilized to highlight the inter-dependencies and predict the future paths of all the subjects jointly. As we focus on real-time applications of our approach, Pishgu is designed to predict a single path ($K = 1$) for each subject. The overall structure of Pishgu can be seen in Figure 1.

3.1. Problem Formulation

Our goal is to predict the future paths of all the subjects in a scene, regardless of the domain of prediction. Keeping that in mind, we use both absolute and relative coordinates as inputs to Pishgu, defined as follows:

$$\mathbf{N}_i = [N_i^{t-T_{in}}, N_i^{t_1-T_{in}}, \dots, N_i^{t_0}] \quad (1)$$

$$\Delta \mathbf{N}_i = [\Delta N_i^{t-T_{in}}, \Delta N_i^{t_1-T_{in}}, \dots, \Delta N_i^{t_0}] \quad (2)$$

where $N_i^t = \langle x_i^t, y_i^t \rangle$ is the position of subject i (vehicle or pedestrian) at time t and T_{in} is number of time steps that model observes for prediction. $\Delta N_i^t = N_i^t - N_i^{t-T_{in}}$ in equation 2 represents the relative coordinates of subject i in time step t with respect to the location of the subject at time step $-T_{in}$.

As mentioned previously, Pishgu predicts a single path for each subject at every time step, and the outputs of the model are formulated as:

$$\hat{\mathbf{Y}}_i = [\hat{Y}_i^{t_1}, \hat{Y}_i^{t_2}, \dots, \hat{Y}_i^{T_{out}}], \quad (3)$$

where \hat{Y}_i^t represents the trajectory of subject i at time t in the future up to T_{out} time steps.

3.2. Architecture

Pishgu’s architecture (see Figure 1) is relatively simple compared to many modern path prediction models. After

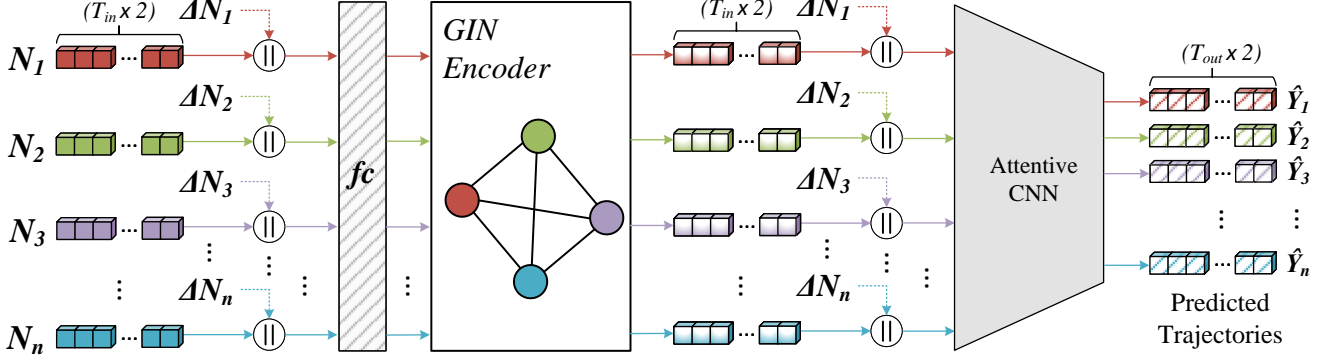


Figure 1. Pishgu formulation visualization. The input N_i refers to a vector of size $T_{in} \times 2$ for each node/subject where T_{in} is the input window size. ΔN_i is the relative vector for each node. fc refers to a fully-connected layer. The output is a $n \times T_{out} \times 2$ matrix, with T_{out} being the output window size. Best seen in color.

the calculation of input features, \mathbf{N} and $\Delta \mathbf{N}$ are concatenated and passed through a single fully-connected layer fc as shown in Figure 1. In the next step, Pishgu leverages a Graph Neural Network (GNN) for embedding the input features. There has been a surge in curiosity towards Graph Neural Networks in recent years because of their power to represent complex interactions, and non-Euclidean data [40, 33, 14]. Many different approaches have been proposed with neighbor aggregation and message passing methods. The final goal of GNNs is to construct a maximally discriminative representation. This means two nodes are mapped to the same location in the embedding space only if they are identical. [40] came up with a simple yet powerful new formulation of GNNs, namely GIN that is shown to be as powerful as the Weisfeiler-Lehman test [15] which is a test that answers the question of whether two graphs are identical or not. We draw motivation from the work of Xu et al. [40] and adapt the network to our specific requirements. Our model constructs a fully connected graph $\mathcal{G} = (\mathcal{V}, \mathcal{E})$ where the nodes (\mathcal{V}) are the subjects of interest present in the frame, and the edges (\mathcal{E}) represent their interactions. The fully connected structure assures that all the possible interactions between subjects are considered, and the network can extract all the important information from other neighbors. Similar to [27, 24], Pishgu utilizes a modified version of aggregation function introduced by [40] and constructs f'_i (the aggregated feature for node i) as follows:

$$f'_i = MLP_0((1 + \theta) \cdot f_i) + MLP_1\left(\sum_{u \in \mathcal{V}(i)} f_j\right) \quad (4)$$

where i is i^{th} subject in the scene, MLP_0 and MLP_1 are Multi-layer Perceptron (MLP) operators each with a single hidden layer, $\mathcal{V}(i)$ is the set of node i neighbors and, θ is a trainable parameter. MLP_0 and MLP_1 are applied to the features of node i and the aggregation of the features from neighbor nodes, respectively. Having two sep-

arate MLPs improves the network’s ability to extract richer features and better integrate neighboring nodes in the context [27]. Keeping the real-time performance in mind, single graph operations is performed across the entire graph, which is enough since the graph is fully connected and all the features can be propagated in one step. Before the final task of path prediction, the output vector of the GIN block (eq. 4) for each subject is concatenated with the respective relative coordinate (eq. 2).

Pishgu makes use of an attentive convolutional neural network for path predictions. It consists of six layers, with each of the three layers of 2D convolution followed by a layer of attention module [37]. The first convolutional layer uses a 2×2 kernel, and the subsequent two convolutional layers use a 2×1 kernel size. The architecture is designed to capture the fast and slow movements of the subjects. The attention module works based on two pillars: channel attention and spatial attention. Channel attention tries to perceive what is essential in the input feature map. To accomplish this task, the channel attention module first performs average pooling and max pooling on the input feature map to encapsulate the input features. These pooling operations improve the module’s efficiency by reducing the feature map size.

In the next step, pooled features are fed to an MLP with one hidden layer to create the channel attention map. The formulation of the channel attention module can be summarized as:

$$\mathbf{AT}_c(\mathbf{F}) = MLP_2(Pool_{avg}(\mathbf{F})) + MLP_2(Pool_{max}(\mathbf{F})) \quad (5)$$

where \mathbf{F} is the input feature map, MLP_2 is an MLP with one hidden layer, and \mathbf{AT}_c is the channel attention module. On the other hand, the goal of the spatial attention module is to locate the important features in the input. For efficiency, average pooling and max pooling are used again, but this time in the channel axis. The pooled features are

concatenated and passed to a convolutional layer for generating the spatial attention map. In summary, the spatial attention module works based on the following equation:

$$\begin{aligned} \mathbf{AT}_s(\mathbf{F}) \\ = \sigma(\text{Conv}^{7 \times 7}([\text{Pool}_{avg}(\mathbf{F}); \text{Pool}_{max}(\mathbf{F})])) \end{aligned} \quad (6)$$

where \mathbf{F} is the input feature map, σ is the sigmoid activation function, $\text{Conv}^{7 \times 7}$ is the convolutional layer with a kernel size of 7, and \mathbf{AT}_c is the spatial attention module.

Incorporating channel attention and spatial attention sequentially has shown significant improvements in the performance of CNNs [38]. Thus, between each convolutional layer, there is an additional module consisting of the channel and spatial attention to improve the predictor’s performance while keeping the network lightweight.

4. Domain Analysis

Challenges and requirements found in path prediction are often domain-specific. The interactions and behaviors vary drastically from predicting a vehicle’s path on a highway with hundreds of vehicles in a scene to predicting the path of a single pedestrian walking on a sidewalk with less than a dozen other people. A general model should be able to adapt across these domains. Thus, understanding each domain’s characteristics is vital in designing a domain-agnostic path prediction model.

Table 1. The statistics of four datasets used for path prediction. These parameters are reported after doing the conventional preprocessing steps discussed in section 4. V_B , P_B , and P_H refer to Vehicle Bird’s-eye view, Pedestrian Bird’s-eye view, and Pedestrian High-angle view respectively. FPS is Frames Per Second.

	NGSIM [5, 6]	ETH [29]	UCY [16]	ActEv/ VIRAT [3]
Domain	V_B	P_B	P_B	P_H
#Subjects	19,698	749	1,456	1,059
#Samples	13.3M	12,035	62,393	130,289
#Frames	108,033	2,044	4,397	41,199
FPS	5	2.5	2.5	2.5

4.1. Vehicle Bird’s-eye View

Most deep learning architectures used for predicting vehicle paths in a highway environment [7, 9, 39] use NGSIM datasets [5, 6]. NGSIM provides complex real-world scenarios and driver behaviors for various traffic patterns. In this paper, we use US-101 [6] and I-80 [5] from NGSIM, each with millions of data samples in bird’s-eye view. Using a bird’s-eye view for path prediction is natural as it provides an overall perspective of the surrounding environment. NGSIM data is collected from cameras mounted on the buildings around the freeways. However, the final

dataset provides the data in bird’s-eye format. This conversion to a bird’s-eye view helps deep learning models learn complicated driver behaviors and their reactions to the surroundings.

4.2. Pedestrian Bird’s-eye View

Two widely used pedestrian path prediction datasets are ETH [29] and UCY [16]. They consist of bird’s-eye view annotations of several crowded scenes with complicated nonlinear pedestrian paths. The position of the pedestrians in these datasets is gathered in real-world coordinates in meters. The data points generally used for training are sampled at a rate of 2.5 Frames Per Second (FPS). ETH looks at two different scenes, ETH and HOTEL, whereas UCY looks at three different scenes, UNIV, ZARA1, and ZARA2. These datasets are especially useful for training models that focus on drone-related applications or environment monitoring. They do not include any data for other points of view such as high-angle or side views.

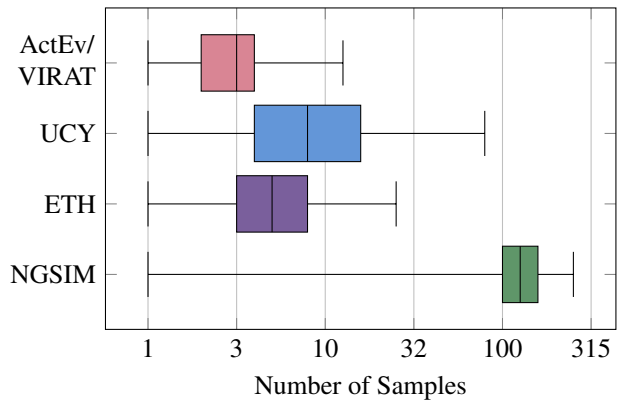


Figure 2. Distribution of number of samples in a frame for ActEv/VIRAT [3], UCY [16], ETH [29] and NGSIM [5, 6] datasets. X axis shows the number of samples in the frame. Please note that the box and whiskers are drawn in logarithmic space for better visualization, and number of samples per each frame can be translated to number of unique subjects in one frame.

4.3. Pedestrian High-angle View

It is unrealistic to assume that a bird’s-eye view angle is always available. Most surveillance cameras are placed at a high location (e.g. the side of a building, on a light pole) to have an overview of the scene from a high-angle view. Thus, path prediction models in real-world scenarios should be able to work with different camera views and angles. Especially if they want to cover normal video surveillance setups. However, most of the works in the path prediction field focus on the bird’s-eye view. On the other hand, in end-to-end real-world environment monitoring and surveillance systems, real-world coordinates are unavailable and the locations of subjects are represented in pixel space. This disconnect between real-world scenarios and most existing

Table 2. Vehicle path prediction error and complexity comparison of Pishgu with contemporary approaches. Second best is underlined.

	RMSE (m)					ADE (m)	FDE (m)	Params (K)
	1s	2s	3s	4s	5s			
CS-LSTM [8]	0.63	1.27	2.09	3.1	4.37	2.29	3.34	191
DeepTrack [12]	0.47	1.08	1.83	2.75	3.89	2.01	3.25	<u>109</u>
GRIP++ [19]	0.38	0.89	1.45	2.14	<u>2.94</u>	1.61	-	-
Pip [32]	0.55	1.18	1.94	2.88	4.04	2.18	-	-
GSTCN [31]	0.44	<u>0.83</u>	<u>1.33</u>	<u>2.01</u>	2.98	<u>1.52</u>	-	49.8
STA-LSTM [23]	<u>0.37</u>	0.98	1.71	2.63	3.78	1.89	<u>3.16</u>	124
Pishgu (Ours)	0.15	0.46	0.82	1.25	1.74	0.88	1.96	132

algorithms makes many proposed methods ill-suited for realistic path prediction. To address this issue, works such as [22, 21, 20, 17] have used ActEv/VIRAT [3] for path prediction. Since then, it has become a standard benchmark for path prediction in pixel space and high-angle view. The primary use of ActEV/VIRAT is activity recognition in challenging real-world scenarios in the surveillance domain. However, the diversity of camera angles and locations in this dataset is advantageous for real-world path prediction as well. Following the same preprocessing steps as Next [22], we downsample the frame rate to 2.5 FPS. The center of the bounding box for a person is used for the extraction of the subject’s locations.

Looking at Table 1, we can see that in the human bird’s-eye view domain, the two publicly available datasets ETH [29] and UCY [16] are relatively small compared to datasets available in other domains. NGSIM [5, 6] has the most number of samples by far and is a much more crowded dataset in terms of the number of samples in each frame. Figure 2 clearly shows that the number of samples in the frame for ETH and UCY datasets is more than ActEv/VIRAT [3], but still much less than the number of samples in NGSIM dataset which even goes up to 248 vehicle in a single frame. Due to these distinctive characteristics that each domain has, a general path prediction method should be able to adapt to each domain to be able to satisfy each domain’s requirements.

5. Experiments

This section evaluates our method for path prediction in all three different domains discussed in Section 4. We compare Pishgu with SotA models in terms of three different error calculations and model sizes. All of the evaluations in this article have been conducted on a server containing Tesla V100 GPU, 2x AMD EPYC 7513 CPUs, and 256GB of RAM. Additionally, latency and throughput through real-time inference are reported on Nvidia Carmel and ARM Cortex-A57 processors.

5.1. Evaluation Metrics

Average Displacement Error (ADE): The average L2 distance between the predicted coordinates (\hat{Y}) and the ground truth coordinates (Y) over all T_{out} predicted time steps and all subjects of interest (N) available in the scene:

$$ADE = \frac{\sum_{i=1}^N \sum_{t=1}^{T_{out}} \|Y_i^t - \hat{Y}_i^t\|_2}{N * T_{out}} \quad (7)$$

Final Displacement Error (FDE): The average L2 distance between the predicted coordinates (\hat{Y}) and the ground truth coordinates (Y) of the last predicted time step over all subjects of interest (N) available in the scene:

$$FDE = \frac{\sum_{i=1}^N \|Y_i^{T_{out}} - \hat{Y}_i^{T_{out}}\|_2}{N} \quad (8)$$

Root Mean Square Error (RMSE): The RMSE at time t is the square root of the mean square error between the predicted path (\hat{Y}) and the ground truth path (Y) of the subjects of interest in the scene:

$$RMSE^t = \sqrt{\frac{1}{N} \sum_{i=1}^N (Y_i^t - \hat{Y}_i^t)^2} \quad (9)$$

We report and compare the complexity of our model against the SotA approaches in terms of number parameters. In Section 5.5, we calculate the latency of prediction per sample in milliseconds and the throughput in FPS.

5.2. Vehicle Bird’s-eye View

Recent works [31, 43, 2] have used the NGSIM public datasets for vehicle path prediction as it provides many complex highway scenarios. The dataset is split into a 70% training set, 10% validation set, and 20% test set. Pishgu has been trained for 40 epochs with a learning rate of 0.01 and the Adam optimizer [13].

As shown in Table 2, we review the performance of Pishgu in terms of RMSE, ADE, FDE, and model size

Table 3. Single-future path prediction error comparison of Pishgu in pedestrian bird’s-eye view domain with contemporary approaches. ADE and FDE are reported in pixel space. Best is in bold text. Second best is underlined.

	ETH		HOTEL		UNIV		ZARA1		ZARA2		AVG		Params (M)
	ADE	FDE											
Linear	1.33	2.94	0.39	0.72	0.82	1.59	0.62	1.21	0.77	1.48	0.79	1.59	-
LSTM	1.09	2.41	0.86	1.91	0.61	1.31	0.41	0.88	0.52	1.11	0.7	1.52	-
Social-LSTM [1]	1.09	2.35	0.79	1.76	0.67	1.4	0.47	1	0.56	1.17	0.72	1.54	-
Next [22]	0.88	1.98	0.36	0.74	0.62	1.32	0.42	0.9	0.34	0.75	0.52	1.14	3.95
CARPe [27]	0.8	1.48	0.52	1	0.61	1.23	0.42	0.84	0.34	0.69	0.54	1.05	0.10
Trajectron++ [30]	0.71	1.66	<u>0.22</u>	<u>0.46</u>	0.44	<u>1.17</u>	0.30	<u>0.79</u>	0.23	<u>0.59</u>	0.38	<u>0.93</u>	-
ScePT [4]	0.19	<u>1.33</u>	0.18	1.12	0.19	1.19	0.18	1.1	<u>0.19</u>	1.2	0.19	1.19	-
SSAGCN [25]	<u>0.30</u>	0.59	<u>0.22</u>	0.42	<u>0.25</u>	0.47	<u>0.20</u>	0.39	0.14	0.28	<u>0.22</u>	0.43	-
Pishgu (Ours)	1.1	2.24	1.17	2.17	0.67	1.37	0.45	0.91	0.36	0.73	0.75	1.48	<u>0.11</u>

Table 4. Experiment results on ActEV/VIRAT [3] dataset. Result are reported in pixel space for single-future path prediction. Best is in bold text. Second best is underlined.

	Social-LSTM [1]	Social-GAN (V) [11]	Social-GAN (PV) [11]	Next [22]	Multiverse [21]	SimAug [20]	ST-MR [17]	Pishgu (Ours)
ADE	23.10	30.40	30.42	19.78	<u>18.51</u>	21.73	18.58	14.11
FDE	44.27	61.93	60.70	42.43	<u>35.84</u>	42.22	36.08	27.96
Params (M)	-	-	-	<u>3.95</u>	-	-	-	0.11

against best in class models [7, 12, 19, 32, 31, 23]. Reporting RMSE is crucial in vehicle path prediction as autonomous vehicles evaluate the future trajectories of surrounding subjects for every second in the future upto few seconds. Pishgu, like the other models, observes the input for 15-time steps (3 seconds) and predicts the path of all the vehicles in a scene for 25-time steps (5 seconds). In terms of RMSE, Pishgu performs better at all the time steps than the other models. It reduces the RMSE by 44%, 38%, and 37% for 2nd, 3rd, and 4th sec as compared to [31]. Compared to best-performing models for 1st and 5th sec, Pishgu reduces the RMSE by 50% and 40%. Similar performance is observed in ADE and FDE, where we improve the SotA error rates by 42% and 61%, respectively. As the majority of the frames in NGSIM are crowded, it helps the attention module to grasp the most important relational behaviors between the subjects for path prediction. Thus, attention module proves to be most effective for NGSIM dataset.

In model size, Pishgu is comparable to most contemporary deep learning models. However, [31] reports less than half the parameters than Pishgu. The smaller size of GSTCN is due to the use of a simple CNN for path prediction and restricting the graph to two laterally adjacent lanes and ± 100 meters. In contrast, Pishgu uses attention-based CNN with a graph of the entire scene to grasp the overall environment provided by the NGSIM dataset.

5.3. Pedestrian Bird’s-eye View

In the pedestrian bird’s-eye view domain, we evaluated our model on ETH [29] and UCY [16], the characteristics of which were detailed in Section 4. We will adapt the same strategy for evaluation as previous works in this domain [11] and train our model with a leave-one-out approach on combined ETH and UCY datasets. As input, the model observes 8 time steps (3.2 seconds) and predicts the coordinates of the pedestrian for the future 12 time steps (4.8 seconds). The model has been trained for 80 epochs with a learning rate of 0.01 and Adam optimizer [13].

In the field of path prediction, it is common for models to generate 20 outputs (k=20) for each subject in the scene and report the ADE and FDE based on the single best of the 20 predicted paths for each pedestrian. However, this method is not suitable for real-time scenarios, especially those deployed on embedded platforms with limited resources. Thus, we will compare our model only to the approaches that report their single-future path prediction evaluation. In our comparisons, we include Linear which is a simple regressor used for path prediction. Another baseline method that we consider is LSTM which is a simple LSTM encoder-decoder model used for path prediction. Table 3 shows that Pishgu struggles with path prediction in this domain. This is due to the fact that ETH[29] and UCY [16] are relatively small datasets and can not provide sufficient amount of training data for the convolution attention mechanism to be trained well as discussed in Section 4.

Table 5. Latency and throughput evaluation on Nvidia Carmel processor and ARM Cortex-A57 processor in milliseconds and FPS respectively. Samples per Frame is an average. FPS is Frames Per Second.

	Sample per Frame	Nvidia Carmel		ARM Cortex-A57	
		Latency (ms)	FPS	Latency (ms)	FPS
Vehicle Bird's-eye View					
NGSIM [5, 6]	158	2.69	2.35	3.50	1.81
Pedestrian Bird's-eye View					
UCY [29]	8	1.44	86.81	2.41	51.81
ETH [16]	3	1.75	190.48	2.06	161.81
Pedestrian High-angle View					
ActEv/VIRAT [3]	5	2.83	70.67	3.4	58.82

We also, report model complexity as number of parameters, but most of the previous works do not examine this crucial factor. Looking at Table 3, we can see that Pishgu has competitive model size compared to CARPe [27] and around $36\times$ smaller model size compare to Next [22].

5.4. Pedestrian High-angle View

Following the previous works [22, 21, 20, 17] we analyze the efficacy of Pishgu by training and testing it on ActEV/VIRAT [3] challenge dataset discussed in Section 4. We report ADE and FDE for evaluating the displacement error. The official training and validation sets have been used for collecting the mentioned evaluation results. As input, the model observes 8 time steps or 3.2 seconds and predicts the path for the future 12 time steps or 4.8 seconds.

We compare our model to other models that do single-future path prediction in this domain since in real-time applications having multiple predicted paths per pedestrian is not realistic. Results reported in pixel space can be seen in Table 4. Social-LSTM [1] and Social-GAN (both V and PV variants) results are based on the tests performed by [22]. Comparison with other approaches makes evident the advantage of Pishgu with a 23.6% and 22.6% decrease in ADE and FDE with respect to the previous SotA model. These results push Pishgu to the top position in single-future path prediction by a large margin and show the benefit of attentive CNN predictor in grasping the meaningful features generated by the GIN in the embedding stage.

In terms of number of parameter, we are only able to compare Pishgu to Next [22] since other works do not mention their model sizes. Pishgu with around $36\times$ smaller model compared to Next and the outstanding ADE and FDE results, is much more suitable for real-time deployment than previous works.

5.5. Real-time Evaluation

Real-time path prediction applications are often implemented on resource-constrained embedded devices. Limited memory, limited power, and real-time implementation make lightweight, low latency models necessary. We report the latency performance of Pishgu on multiple embedded processors; the 15W dual-core Nvidia Carmel processor with 8GB of RAM and the 10W quad-core ARM Cortex-A57 processor with 2GB of RAM. We report the performance of two embedded processors to demonstrate the adaptability of Pishgu in different resource-constrained environments. Both processors are utilized at their respective highest power capacities. All the results on embedded processors are calculated for the batch size of one. We test Pishgu for all three domains and report the latency per subject in milliseconds (ms) and throughput in terms of FPS.

The number of samples per frame is utilized to calculate the throughput to demonstrate the performance of Pishgu in real-world, real-time applications. As shown in Table 5, high numbers of vehicles in each frame of the NGSIM datasets ensure dense graphs, and millions of data samples help attention mechanism in feature map refinement [37]. However, the number of path predictions for the NGSIM dataset using Pishgu goes to more than 200 vehicles for a single frame. This, in turn, affects the overall throughput of the model even with low latency per sample. As the number of samples per frame for all the other datasets is meager compared to NGSIM, the throughput for other datasets is considerably higher.

The throughput of NGSIM for the Nvidia Carmel processor is 2.35 FPS which is 29.83% better than 1.81 FPS for the lower-power ARM Cortex processor. Similarly for pedestrian tracking, the throughput for UCY [29], ETH [16], and ActEv/VIRAT [3] on the Nvidia Carmel is 67.55%, 17.72%, and 20.15% better than that on ARM Cortex based embedded platform respectively. The superior performance of the Carmel processor can be credited to a higher operating power capacity of 15W with a higher clock frequency of 1.9 GHz. On the other hand, the ARM cortex with quad-core operates at 10W with a frequency of 1.5 GHz. Higher power distribution among the dual-core of Carmel processors also plays a role in justifying its performance. The average latency per sample for vehicle bird's-eye view on Nvidia Carmel Processor is 2.69 ms, which is 23% better than that of the ARM Cortex processor. Similar trends are observed in all the latency improvements comparison between two processors in pedestrian bird's-eye and high-angle view datasets. Hence, we demonstrate that Pishgu can be utilized in real-world applications using embedded processors on off-the-shelf platforms with suitable latency and throughput performance.

6. Conclusion

In this paper, we propose Pishgu, a domain agnostic path prediction model that leverages graph isomorphism networks and attention mechanisms. We evaluate the competency of our model in three domains and present extensive domain analysis with their effects on the performance of our model in terms of error and model size. Moreover, Pishgu brings path prediction one step closer to real-world applications, performing in real-time on embedded processors. Pishgu achieves SotA performance for path prediction in vehicle bird's-eye and pedestrian high-angle view domains on NGSIM and ActEV/VIRAT, respectively, by a considerable margin.

References

- [1] Alexandre Alahi, Kratarth Goel, Vignesh Ramanathan, Alexandre Robicquet, Li Fei-Fei, and Silvio Savarese. Social lstm: Human trajectory prediction in crowded spaces. In *Proceedings of the IEEE conference on computer vision and pattern recognition*, pages 961–971, 2016.
- [2] Jiyao An, Wei Liu, Qingqin Liu, Liang Guo, Ping Ren, and Tao Li. Dgnet: Dynamic graph and interaction-aware convolutional network for vehicle trajectory prediction. *Neural Networks*, 151:336–348, 2022.
- [3] TRECVID Awad George. Benchmarking video activity detection, video captioning and matching, video storytelling linking and video search. In *Proceedings of TRECVID*, 2018.
- [4] Yuxiao Chen, Boris Ivanovic, and Marco Pavone. Scept: Scene-consistent, policy-based trajectory predictions for planning. In *Proceedings of the IEEE/CVF Conference on Computer Vision and Pattern Recognition*, pages 17103–17112, 2022.
- [5] James Colyar and John Halkias. Next generation simulation (NGSIM), Interstate 80 freeway dataset. FHWA-HRT-06-137, 2006.
- [6] James Colyar and John Halkias. Next generation simulation (NGSIM), US Highway-101 dataset. FHWA-HRT-07-030., 2007.
- [7] Nachiket Deo and Mohan M. Trivedi. Convolutional social pooling for vehicle trajectory prediction. *CoRR*, abs/1805.06771, 2018.
- [8] Nachiket Deo and Mohan M. Trivedi. Convolutional social pooling for vehicle trajectory prediction. In *2018 IEEE Conference on Computer Vision and Pattern Recognition Workshops, CVPR Workshops 2018, Salt Lake City, UT, USA, June 18-22, 2018*, pages 1468–1476. Computer Vision Foundation / IEEE Computer Society, 2018.
- [9] Mengyin Fu, Ting Zhang, Wenjie Song, Yi Yang, and Meiling Wang. Trajectory prediction-based local spatio-temporal navigation map for autonomous driving in dynamic highway environments. *IEEE Trans. Intell. Transp. Syst.*, 23(7):6418–6429, 2022.
- [10] Harris Georgiou, Sophia Karagiorgou, Yannis Kontoulis, Nikos Pelekis, Petros Petrou, David Scarlatti, and Yannis Theodoridis. Moving objects analytics: Survey on future location & trajectory prediction methods. *arXiv preprint arXiv:1807.04639*, 2018.
- [11] Agrim Gupta, Justin Johnson, Li Fei-Fei, Silvio Savarese, and Alexandre Alahi. Social gan: Socially acceptable trajectories with generative adversarial networks. In *Proceedings of the IEEE conference on computer vision and pattern recognition*, pages 2255–2264, 2018.
- [12] Vinit Katariya, Mohammadreza Baharani, Nichole Morris, Omidreza Shoghli, and Hamed Tabkhi. Deeptrack: Lightweight deep learning for vehicle trajectory prediction in highways. *IEEE Transactions on Intelligent Transportation Systems*, pages 1–10, 2022.
- [13] Diederik P Kingma and Jimmy Ba. Adam: A method for stochastic optimization. *arXiv preprint arXiv:1412.6980*, 2014.
- [14] Thomas N Kipf and Max Welling. Semi-supervised classification with graph convolutional networks. *arXiv preprint arXiv:1609.02907*, 2016.
- [15] AA Leman and Boris Weisfeiler. A reduction of a graph to a canonical form and an algebra arising during this reduction. *Nauchno-Tekhnicheskaya Informatsiya*, 2(9):12–16, 1968.
- [16] Alon Lerner, Yiorgos Chrysanthou, and Dani Lischinski. Crowds by example. In *Computer graphics forum*, volume 26, pages 655–664. Wiley Online Library, 2007.
- [17] Lihuan Li, Maurice Pagnucco, and Yang Song. Graph-based spatial transformer with memory replay for multi-future pedestrian trajectory prediction. In *Proceedings of the IEEE/CVF Conference on Computer Vision and Pattern Recognition*, pages 2231–2241, 2022.
- [18] Xin Li, Xiaowen Ying, and Mooi Choo Chuah. GRIP: graph-based interaction-aware trajectory prediction. In *2019 IEEE Intelligent Transportation Systems Conference, ITSC 2019, Auckland, New Zealand, October 27-30, 2019*, pages 3960–3966. IEEE, 2019.
- [19] Xin Li, Xiaowen Ying, and Mooi Choo Chuah. Grip++: Enhanced graph-based interaction-aware trajectory prediction for autonomous driving. *arXiv preprint arXiv:1907.07792*, 2020.
- [20] Junwei Liang, Lu Jiang, and Alexander Hauptmann. Simaug: Learning robust representations from simulation for trajectory prediction. In *European Conference on Computer Vision*, pages 275–292. Springer, 2020.
- [21] Junwei Liang, Lu Jiang, Kevin Murphy, Ting Yu, and Alexander Hauptmann. The garden of forking paths: Towards multi-future trajectory prediction. In *Proceedings of the IEEE/CVF Conference on Computer Vision and Pattern Recognition*, pages 10508–10518, 2020.
- [22] Junwei Liang, Lu Jiang, Juan Carlos Niebles, Alexander G Hauptmann, and Li Fei-Fei. Peeking into the future: Predicting future person activities and locations in videos. In *Proceedings of the IEEE/CVF conference on computer vision and pattern recognition*, pages 5725–5734, 2019.
- [23] Lei Lin, Weizi Li, Huikun Bi, and Lingqiao Qin. Vehicle trajectory prediction using lstms with spatial-temporal attention mechanisms. *IEEE Intell. Transp. Syst. Mag.*, 14(2):197–208, 2022.
- [24] Yongkang Liu, Xuewei Qi, Emrah Akin Sisbot, and Kentaro Oguchi. Multi-agent trajectory prediction with graph attention isomorphism neural network. In *2022 IEEE Intelligent Vehicles Symposium (IV)*, pages 273–279. IEEE, 2022.
- [25] Pei Lv, Wentong Wang, Yunxin Wang, Yuzhen Zhang, Mingliang Xu, and Changsheng Xu. Ssagcn: Social soft attention graph convolution network for pedestrian trajectory prediction. *arXiv preprint arXiv:2112.02459*, 2021.
- [26] Karttikeya Mangalam, Yang An, Harshayu Girase, and Jitendra Malik. From goals, waypoints & paths to long term human trajectory forecasting. In *Proceedings of the IEEE/CVF International Conference on Computer Vision*, pages 15233–15242, 2021.
- [27] Matías Mendieta and Hamed Tabkhi. Carpe posterum: A convolutional approach for real-time pedestrian path prediction. In *Proceedings of the AAAI Conference on Artificial Intelligence*, volume 35, pages 2346–2354, 2021.

- [28] Xiaoyu Mo, Zhiyu Huang, Yang Xing, and Chen Lv. Multi-agent trajectory prediction with heterogeneous edge-enhanced graph attention network. *IEEE Transactions on Intelligent Transportation Systems*, 23(7):9554–9567, 2022.
- [29] Stefano Pellegrini, Andreas Ess, Konrad Schindler, and Luc Van Gool. You’ll never walk alone: Modeling social behavior for multi-target tracking. In *2009 IEEE 12th international conference on computer vision*, pages 261–268. IEEE, 2009.
- [30] Tim Salzmann, Boris Ivanovic, Punarjay Chakravarty, and Marco Pavone. Trajectron++: Dynamically-feasible trajectory forecasting with heterogeneous data. In *European Conference on Computer Vision*, pages 683–700. Springer, 2020.
- [31] Zihao Sheng, Yunwen Xu, Shibe Xue, and Dewei Li. Graph-based spatial-temporal convolutional network for vehicle trajectory prediction in autonomous driving. *CoRR*, abs/2109.12764, 2021.
- [32] Haoran Song, Wenchao Ding, Yuxuan Chen, Shaojie Shen, Michael Yu Wang, and Qifeng Chen. Pip: Planning-informed trajectory prediction for autonomous driving. In Andrea Vedaldi, Horst Bischof, Thomas Brox, and Jan-Michael Frahm, editors, *Computer Vision - ECCV 2020 - 16th European Conference, Glasgow, UK, August 23-28, 2020, Proceedings, Part XXI*, volume 12366 of *Lecture Notes in Computer Science*, pages 598–614. Springer, 2020.
- [33] Petar Veličković, Guillem Cucurull, Arantxa Casanova, Adriana Romero, Pietro Lio, and Yoshua Bengio. Graph attention networks. *arXiv preprint arXiv:1710.10903*, 2017.
- [34] Anirudh Vemula, Katharina Muelling, and Jean Oh. Social attention: Modeling attention in human crowds, 2017.
- [35] Chujie Wang, Lin Ma, Rongpeng Li, Tariq S Durrani, and Honggang Zhang. Exploring trajectory prediction through machine learning methods. *IEEE Access*, 7:101441–101452, 2019.
- [36] Conghao Wong, Beihao Xia, Ziming Hong, Qinmu Peng, and Xinge You. View vertically: A hierarchical network for trajectory prediction via fourier spectrums. *arXiv preprint arXiv:2110.07288*, 2021.
- [37] Sanghyun Woo, Jongchan Park, Joon-Young Lee, and In So Kweon. CBAM: convolutional block attention module. In Vittorio Ferrari, Martial Hebert, Cristian Sminchisescu, and Yair Weiss, editors, *Computer Vision - ECCV 2018 - 15th European Conference, Munich, Germany, September 8-14, 2018, Proceedings, Part VII*, volume 11211 of *Lecture Notes in Computer Science*, pages 3–19. Springer, 2018.
- [38] Sanghyun Woo, Jongchan Park, Joon-Young Lee, and In So Kweon. Cbam: Convolutional block attention module. In *Proceedings of the European conference on computer vision (ECCV)*, pages 3–19, 2018.
- [39] Xu Xie, Chi Zhang, Yixin Zhu, Ying Nian Wu, and Song-Chun Zhu. Congestion-aware multi-agent trajectory prediction for collision avoidance. In *IEEE International Conference on Robotics and Automation, ICRA 2021, Xi’an, China, May 30 - June 5, 2021*, pages 13693–13700. IEEE, 2021.
- [40] Keyulu Xu, Weihua Hu, Jure Leskovec, and Stefanie Jegelka. How powerful are graph neural networks? *arXiv preprint arXiv:1810.00826*, 2018.
- [41] Luyao Ye, Zezhong Wang, Xinhong Chen, Jianping Wang, Kui Wu, and Kejie Lu. Gsan: Graph self-attention network for learning spatial-temporal interaction representation in autonomous driving. *IEEE Internet of Things Journal*, 9(12):9190–9204, 2022.
- [42] Jiangbei Yue, Dinesh Manocha, and He Wang. Human trajectory prediction via neural social physics. *arXiv preprint arXiv:2207.10435*, 2022.
- [43] Kunpeng Zhang, Liang Zhao, Chengxiang Dong, Lan Wu, and Liang Zheng. Ai-tp: Attention-based interaction-aware trajectory prediction for autonomous driving. *IEEE Transactions on Intelligent Vehicles*, 2022.
- [44] Hao Zhou, Dongchun Ren, Xu Yang, Mingyu Fan, and Hai Huang. Sliding sequential cvae with time variant socially-aware rethinking for trajectory prediction. *arXiv preprint arXiv:2110.15016*, 2021.